

**STUDY ON THE EFFECTS OF TiO<sub>2</sub> DOPING ON PURE SnO<sub>2</sub> FOR ETHANOL  
GAS SENSING PROPERTIES.**

**PAVINTHRAN A/L MARAN**

**UNIVERSITI SAINS MALAYSIA**

**2017**

**STUDY ON THE EFFECTS OF TiO<sub>2</sub> DOPING ON PURE SnO<sub>2</sub> FOR ETHANOL  
GAS SENSING PROPERTIES.**

**by**

**PAVINTHRAN A/L MARAN**

**This thesis submitted in partial fulfillment of the requirements for the degree of  
Bachelor of Chemical Engineering.**

**June 2017**

## **ACKNOWLEDGEMENT**

First and foremost, I would like to convey my sincere gratitude to my supervisor, Associate Professor Dr. Mohamad Zailani Abu Bakar for his precious encouragement, guidance and generous support throughout this work.

I would also extend my gratitude towards all my colleagues for their kindness cooperation and helping hands in guiding me carrying out the lab experiment. They are willing to sacrifice their time in guiding and helping me throughout the experiment besides sharing their valuable knowledge.

Apart from that, I would also like to thank all SCE staffs for their kindness cooperation and helping hands. Indeed, their willingness in sharing ideas, knowledge and skills are deeply appreciated.

Once again, I would like to thank all the people, including those whom I might have missed out and my friends who have helped me directly or indirectly. Their contributions are very much appreciated. Thank you very much.

*PAVINTHRAN MARAN*

*MAY 2017*

## TABLE OF CONTENTS

	<b>Page</b>
<b>ACKNOWLEDGEMENT</b>	<b>ii</b>
<b>TABLE OF CONTENTS</b>	<b>iii</b>
<b>LIST OF FIGURES</b>	<b>v</b>
<b>LIST OF TABLES</b>	<b>vii</b>
<b>LIST OF ABBREVIATION</b>	<b>viii</b>
<b>ABSTRAK</b>	<b>ix</b>
<b>ABSTRACT</b>	<b>x</b>
<b>CHAPTER ONE : INTRODUCTION</b>	
1.1 Research background	1
1.2 Problem Statement	4
1.3 Research objectives	5
1.4 Scope of study	6
<b>CHAPTER TWO : LITERATURE REVIEW</b>	
2.1 Introduction	7
2.2 Band theory of semiconductor n-type metal oxide sensors (SMO)	7
2.3 Effect of TiO <sub>2</sub> wt% doping on SnO <sub>2</sub> on ethanol vapor concentration	9
2.4 Effect of TiO <sub>2</sub> wt% doping on pure SnO <sub>2</sub> on different humidity of ethanol vapor	11
2.5 Effect of TiO <sub>2</sub> wt% doping on pure SnO <sub>2</sub> on operating temperature of ethanol vapor	13
2.6 Screen-printing method	14
2.7 Sol-gel and co-precipitation method	15
<b>CHAPTER THREE : MATERIALS AND METHODS</b>	
3.1 Experimental flow chart	16
3.2 Material	17

3.3	Active material synthesis	17
3.3.1	Preparation of TiO <sub>2</sub> doped SnO <sub>2</sub> powder	17
3.3.2	Preparation of pure SnO <sub>2</sub> powder.	18
3.4	Preparation of pure SnO <sub>2</sub> and Ti doped SnO <sub>2</sub> thick film ethanol gas sensor.	19
3.5	Experimental design	20
3.6	Equipment and Instrument	20
3.6.1	Sensor characterization	20
3.6.1(a)	X-Ray Diffraction (XRD)	20
3.6.2	Sensor Measurement Unit	21
CHAPTER FOUR : RESULTS AND DISCUSSIONS		
4.1	Introduction	23
4.2	Sensor characterization	23
4.2.1	X-Ray Diffraction (X-Ray) analysis	23
4.3	Determination of optimum parameters value	25
4.3.1	Operating temperature of ethanol	25
4.3.2	Concentration of ethanol	33
CHAPTER FIVE : CONCLUSIONS AND RECOMMENDATIONS		
5.1	Conclusion	39
5.2	Recommendations	40
REFERENCE		41

## LIST OF FIGURES

		PAGE
Figure 2.1	Energy-band diagram for the TiO <sub>2</sub> -SnO <sub>2</sub> composite System	8
Figure 2.2	Physical form of screen-printed SMO gas sensors	14
Figure 3.1	(a) Semi-auto screen printing machine. (b) Mesh screen	19
Figure 3.2	Schematic diagram of the gas sensor rig.	22
Figure 3.3	Actual set-up of sensor measurement rig.	22
Figure 4.1	XRD patterns of the samples: (a) 60 wt% TiO <sub>2</sub> -40 wt% SnO <sub>2</sub> , (b) 40 wt% TiO <sub>2</sub> -60 wt% SnO <sub>2</sub> , (c) 20 wt% TiO <sub>2</sub> -80 wt% SnO <sub>2</sub> , (d) Pure SnO <sub>2</sub> .	23
Figure 4.2	Dynamic changes of electrical resistance for pure SnO <sub>2</sub>	25
Figure 4.3	Dynamic changes of electrical resistance for 20 wt% TiO <sub>2</sub> -80 wt% SnO <sub>2</sub>	26
Figure 4.4	Dynamic changes of electrical resistance for 40 wt% TiO <sub>2</sub> -60 wt% SnO <sub>2</sub>	27
Figure 4.5	Dynamic changes of electrical resistance for 60 wt% TiO <sub>2</sub> -40 wt% SnO <sub>2</sub>	28
Figure 4.6	Variation in response as a function of operating temperature for the sensors towards ethanol at 1000 ppm.	29
Figure 4.7	Dynamic changes of electrical resistance for pure SnO <sub>2</sub>	33
Figure 4.8	Dynamic changes of electrical resistance for 20 wt% TiO <sub>2</sub> -80 wt% SnO <sub>2</sub>	34
Figure 4.9	Dynamic changes of electrical resistance for 40 wt% TiO <sub>2</sub> -60 wt% SnO <sub>2</sub>	35
Figure 4.10	Dynamic changes of electrical resistance for 60 wt% TiO <sub>2</sub> -40 wt% SnO <sub>2</sub>	36

Figure 4.11 Variation in response as a function of ethanol gas concentration for the sensors towards ethanol at their respective optimum temperatures.

37

## LIST OF TABLES

		PAGE
Table 3.1	Specification of material used	17
Table 3.2	Different TiO <sub>2</sub> wt% doping on SnO <sub>2</sub> powder Synthesized	18
Table 4.1	Crystallite size of samples using Rietveld refinement	24
Table 4.2	Response-recovery time of all the samples at their respective temperatures.	31



## LIST OF ABBREVIATION

XRD	X-Ray Powder diffraction
VOC	Volatile Organic Compound
BAC	Blood Alcohol Concentration
wt%	Weight percentage
$R_{\text{air}}$	Resistance of air (ohm)
$R_{\text{gas}}$	Resistance of gas (ohm)
S	Sensitivity

**KAJIAN MENGENAI KESAN KEMADATAN  $\text{TiO}_2$  PADA  $\text{SnO}_2$  TULEN  
UNTUK KEPEKAAN TERHADAP GAS ETANOL.**

**ABSTRAK**

Tujuan kajian ini adalah untuk mengkaji mengenai kesan kemadatan pelbagai peratusan berat  $\text{TiO}_2$  pada  $\text{SnO}_2$  untuk penderiaan gas etanol. Tiga peratusan berat  $\text{TiO}_2$  iaitu 20, 40 dan 60% pada  $\text{SnO}_2$  tulen disintesis melalui kaedah pemendakan, manakala serbuk  $\text{SnO}_2$  tulen disintesis melalui kaedah sol-gel. Lapisan serbuk aktif kemudiannya disapukan di atas permukaan 10mm x 10mm substrat aluminat melalui kaedah percetakan skrin. Sampel-sampel telah dicirikan oleh Pembelauan Serbuk X-Ray (XRD). Semua sampel telah diuji dengan suhu yang berbeza daripada 150°C hingga 450°C pada kepekatan etanol 1000ppm. Suhu optimum untuk setiap sampel telah ditentukan melihat suhu yang mempamerkan prestasi kepekaan dan tindak balas pemulihan masa yang terbaik. Sensor-sensor kemudiannya telah diuji dengan variasi etanol kepekatan gas yang terdiri daripada 150ppm hingga 1000ppm pada suhu optimum masing-masing. Sampel  $\text{SnO}_2$  tulen menunjukkan kepekaan maksimum sebanyak 29.76 pada 350°C, dan merupakan yang tertinggi dalam kalangan semua sampel. Masa tindak balas sampel adalah 7s, yang terendah dalam kalangan semua sampel dan merekodkan masa pemulihan tertinggi sebanyak 99s, tertinggi dalam kalangan semua sampel kerana rintangan asas rendah dicapai. Apabila diuji dengan perubahan kepekatan gas etanol,  $\text{SnO}_2$  tulen mempamerkan kepekaan maksimum sebanyak 49.03 pada 1000ppm.  $\text{SnO}_2$  tulen kekal menjadi sensor yang sesuai untuk pelbagai suhu dari 250°C hingga 350°C dan untuk kepekatan etanol, dari 150ppm hingga 1000ppm berbanding sensor  $\text{TiO}_2$  serap  $\text{SnO}_2$ .

# **STUDY ON THE EFFECTS OF TiO<sub>2</sub> DOPING ON PURE SnO<sub>2</sub> FOR ETHANOL GAS SENSING PROPERTIES.**

## **ABSTRACT**

The aim of this research is to study on the effects of different TiO<sub>2</sub> weight % doping on SnO<sub>2</sub> ethanol gas sensing properties. Three different TiO<sub>2</sub> weight % doping of 20, 40 and 60 wt% on pure SnO<sub>2</sub> are synthesized via precipitation method, while pure SnO<sub>2</sub> powder is synthesized via sol-gel method. The active layer is then deposited on 10mm x 10mm aluminate substrate via screen printing method. The samples have been characterized by X-Ray Powder Diffraction (XRD). All the samples are tested with different temperatures ranging from 150°C to 450°C at ethanol concentration of 1000ppm. The optimum temperature for each samples are obtained by determining temperature the sensors exhibit highest gas sensing performance in terms of sensitivity and response-recovery time. The sensors are then tested in variation of ethanol gas concentration ranging from 150ppm to 1000ppm at respective optimum temperature. Pure SnO<sub>2</sub> sample showed maximum response of 29.76 at 350°C, which is the highest among all the samples. In addition, the response time is 7s, the lowest among all the samples and records the highest recovery time of 99s among all samples due to lowest baseline resistance achieved. When tested with variation of ethanol gas concentration, pure SnO<sub>2</sub> exhibits maximum response of 49.03 at 1000 ppm. Pure SnO<sub>2</sub> active material remains the ideal sensor for temperature range of 250°C to 350°C and 150ppm to 1000ppm for ethanol temperature range compared to hetero structure (TiO<sub>2</sub> doped SnO<sub>2</sub>) sensor

## **CHAPTER ONE**

### **INTRODUCTION**

#### 1.1 Research Background

The demand for compact, robust, with versatile applications and a low cost gas sensor has increased drastically over the years in line with advancement in technology that has propelled various industries in manufacturing and energy sector into greater strides. The role of gas sensors appears to be more relevant in monitoring and controlling systems, whereby, highly precised detection of chemical pollutants such as NO, SO, HCl, CO, volatile organic compounds (VOCs) and fluorocarbon emission source with quantitative data is needed in order to oblige to stricter environmental regulations and to minimize potential explosion or flammability hazards. The functionality of gas sensors is essential to minimize global environmental issues such as the greenhouse effect, acid rain, and ozone depletion.

Analytic instruments such as gas chromatography and optical spectroscopy remains secondary measure to vapor / pollutant detection due to being time consuming and expensive, although these instruments are able to provide accurate analysis. For being gas sensors getting first node in vapor detection system, many researches and study are dedicated in producing high thermal and chemical stability gas sensors that could provide high sensitivity in detecting variety of analytes in most challenging conditions (Lee and Lee, 2001).

Sensors are diversified into solid electrolyte detectors, catalytic detectors, electrochemical detectors, infrared gas detectors, solid-state sensors and paramagnetic

gas sensors, however, this paper narrows its study on solid-state/semiconductor sensors (Jayaweera et al., 2014).

Semiconductor gas sensors are frequently used for detecting inflammable gases and certain toxic gases in air and basically utilize pure metal oxides such Tin (IV) Oxide,  $\text{SnO}_2$  and Zinc (II) Oxide,  $\text{ZnO}$  or noble metal such as Palladium (Pd) and Titanium (Ti) doped on the metal oxides that act as active material in detecting gases.

The gas detection process occurs mainly on active material (metal oxides) sensor surface, that results in the variation of concentration of adsorbed oxygen. Oxygen molecules surrounding the active material surface are chemisorbed, whereby Oxygen ions adsorb onto the material's surface, removing electrons from the bulk, thus creating a potential barrier that minimizes the electron movement and conductivity. When targeted gases combine with this oxygen, the height of the barrier is reduced, increasing conductivity. The change in conductivity is indicates the amount of targeted gas present in the environment, allowing quantitative determination of targeted gas.

The experiment focuses on the detection of ethanol vapor. Detection of ethanol vapor is highly being given attention in this research due to its enormous contribution in many fields. Detection of ethanol vapor is highly crucial in monitoring of ethanol in person's breath is used for measurement blood alcohol concentration (BAC). BAC of 0.08 is the maximum limit, in which the driver alcohol intoxication level should be within for him to be eligible for driving. BAC 0.08 in detailed term would be 0.08 g of alcohol per 100mL of blood, and in any case one's BAC is beyond 0.08, he is forbidden

to drive which can prevent road accidents (Win, 2006). A need for ethanol detection is required in utilizing bioethanol to be blend with gasoline for fuel. Despite being renewable source, bioethanol possess high corrosion towards stainless steel and other metals/alloy, that along the time, experiences leakage. Thus, a proper leak detection mechanism is integrated in vehicles to minimize wastage in fuel and eliminate fire hazard (Fong et al., 2014).

In the research of this paper, SnO<sub>2</sub> based active materials is chosen due to its various gas sensing application used apart from all the metal oxides because of its sensitivity and chemical stability towards volatile organic compounds (VOCs). SnO<sub>2</sub> is an n-type metal oxide in its pure form (Fang and Lee, 1989). However, SnO<sub>2</sub> gas sensors produces weak sensor output when tested with low gas concentration compared to metal oxide or noble metal doped SnO<sub>2</sub>. This is mostly due to larger grain size pure SnO<sub>2</sub> possess with smaller specific surface area for adsorption of O<sub>2</sub> to occur on the surface, meanwhile, the doping of foreign metal oxide or noble metal halts the growing of grain, thus provide a larger specific surface area (Zeng et al., 2010; Chikhale et al., 2014). Furthermore, SnO<sub>2</sub> is found to be thermally unstable and experiences degeneration in electrical properties upon prolonged thermal treatment in reducing the gas atmosphere, thus exhibits poor sensing performance (>400°C) (Vaezi et al., 2012). TiO<sub>2</sub> doping to SnO<sub>2</sub> is seen as the best fit as TiO<sub>2</sub> has minimum cross selectivity towards humidity and stable at higher temperatures (Tricoli et al., 2009; Vaezi et al., 2012). TiO<sub>2</sub> disadvantages of lower sensitivity and conductivity is thereby compensated by excellent gas sensing properties of SnO<sub>2</sub>.

## 1.2 Problem Statement

The most common way in categorizing gas leak detection methods is based on the technical nature, whereby it is split into hardware, software and biological method. Biological method in gas leak detection entirely depends on smell, visual and hearing sense of personnel or more preferably canines stationed along pipelines. However, major disadvantages that lie in this method are inability for long duration conduct due to higher possibility of dangerous amount of toxic gas inhalation and lower credibility in obtained data due to misconception that could arise along the conveying information line. The software method depends on software programs that are integrated with specific algorithms, responsible in monitoring the state of pressure, temperature, flow rate or other pipeline parameters. These numerical data are then interpreted by the algorithms to determine the occurrence of a leak. Analytic instruments such as gas chromatography and optical spectroscopy falls into these categories, however these methods remains secondary measure to vapor / pollutant detection due to being time consuming, requires trained personnel and expensive. Hardware method, meanwhile utilizes the usage of special sensing devices that could be further break down into acoustic, optical, cable sensor, soil monitoring, ultrasonic flow meters and vapor sampling. Although these sensors perform gas detection with distinguished mechanism and working principle, the disadvantages more alike look similar with high cost and difficulties in installation, especially in underground pipelines, frequent interference of external disturbance on obtained data, questioning the credibility of data and weak in determining leak size. Nevertheless, semiconductor sensors have arisen over the discussed methods due to faster response and higher sensibility towards target gas (Murvaya and Sileaa, 2011).

Although SnO<sub>2</sub> gas sensor has higher sensitivity and conductivity towards ethanol, SnO<sub>2</sub> produces weaker sensor output for low concentration of gas due to lower interaction of gas molecules in smaller specific surface area. Besides, SnO<sub>2</sub> is thermally unstable and has poor sensing properties beyond operating temperature of 400°C. Doping of TiO<sub>2</sub> on SnO<sub>2</sub> via TiO<sub>2</sub>-SnO<sub>2</sub> sol gel method minimizes growth of grain, thus increasing specific surface area for surface interaction with target gases. High thermal resistance property of TiO<sub>2</sub> drastically improves the thermal stability of the hetero structure sensor. However, right quantity of TiO<sub>2</sub> doping onto SnO<sub>2</sub> has to be determined so both specific surface area and stability towards higher working temperature parameter is balanced with the band gap energy that reduces with the increment of TiO<sub>2</sub> wt% doping. Reduction in band gap energy reduces the conductivity of active material on ethanol vapor.

### 1.3 Research Objectives

- 1) To study the difference between pure SnO<sub>2</sub> active material and TiO<sub>2</sub> doped SnO<sub>2</sub> and the effects of TiO<sub>2</sub> wt% doping on pure SnO<sub>2</sub> on sensitivity in wide ranges of concentration of ethanol gas (ppm) and operating temperature of ethanol stream.
- 2) To characterize the active materials prepared in terms of crystallite size and phase the chemical compound is present on sensor surface.



#### 1.4 Scope of Study

Hence, the aim of this work is to study the gas sensing properties of pure SnO<sub>2</sub> and TiO<sub>2</sub> wt% doping on pure SnO<sub>2</sub> of 20, 40 and 60%. All the synthesized samples are under in sensor measurement unit using ethanol gas with variation in operating temperature (°C) and concentration of ethanol gas (ppm). The tested operating temperatures are 150°C, 250°C, 350°C and 450°C, while the tested gas concentration is 150ppm, 400ppm, 700ppm, 1000ppm. The study focuses on the effect and amount of doping of foreign metal oxide (TiO<sub>2</sub> doped on SnO<sub>2</sub>) on the working/operating temperature and concentration of the ethanol gas. The pure SnO<sub>2</sub> is prepared via co-precipitation method using stannic chloride, SnCl<sub>4</sub>.5H<sub>2</sub>O, while, Ti doped SnO<sub>2</sub> is prepared via sol-gel method, whereby, stannic chloride, SnCl<sub>4</sub>.5H<sub>2</sub>O acts as tin precursor, with commercial titania powder. Both active material powders are then mixed with organic binder to be formed as paste for screen printing process on the aluminate substrate. The paste is printed in five layers for each substrate. X-ray diffraction (XRD) was used to characterize the microstructure of pure SnO<sub>2</sub> and TiO<sub>2</sub> doped SnO<sub>2</sub> gas-sensing films.

## CHAPTER TWO

### LITERATURE REVIEW

#### 2.1 Introduction

Metal oxides such as  $\text{SnO}_2$ ,  $\text{ZnO}_2$  and  $\text{TiO}_2$  are actively utilized in the semiconductor industry when it comes in manufacturing gas sensors. Tin oxide ( $\text{SnO}_2$ ) is chosen for study in this paper due to its extensive use in rapid detection of chemical vapors due to high integration of  $\text{SnO}_2$  based transducers in monolithic micro-systems. Besides,  $\text{SnO}_2$  based active materials possess high sensitivity towards several target vapors down to ppb concentrations. Throughout the years, the morphology of  $\text{SnO}_2$  Nano crystals has been finely tuned due to the higher prospect in increasing lower detection limit, sensitivity and long term stability.

#### 2.2 Band theory of semiconductor n-type metal oxide sensors (SMO)

Band theory explains about the interaction of target gas with the surface of the metal oxide film (generally through surface adsorbed oxygen ions). The interaction alters the charge carrier concentration of the material that further changes the conductivity (or resistivity,) of the material (Fine et al., 2010). The use of  $\text{TiO}_2$  is justified due to formation of n-n hetero junctions between  $\text{TiO}_2$  and  $\text{SnO}_2$  that forms large difference in band gap between  $\text{TiO}_2$  (3.2eV) and  $\text{SnO}_2$  (3.6eV) that increases the rate of electron transfer from  $\text{TiO}_2$  to  $\text{SnO}_2$  due to conduction band edge of  $\text{TiO}_2$  lies above that of  $\text{SnO}_2$  as shown in the figure next page.

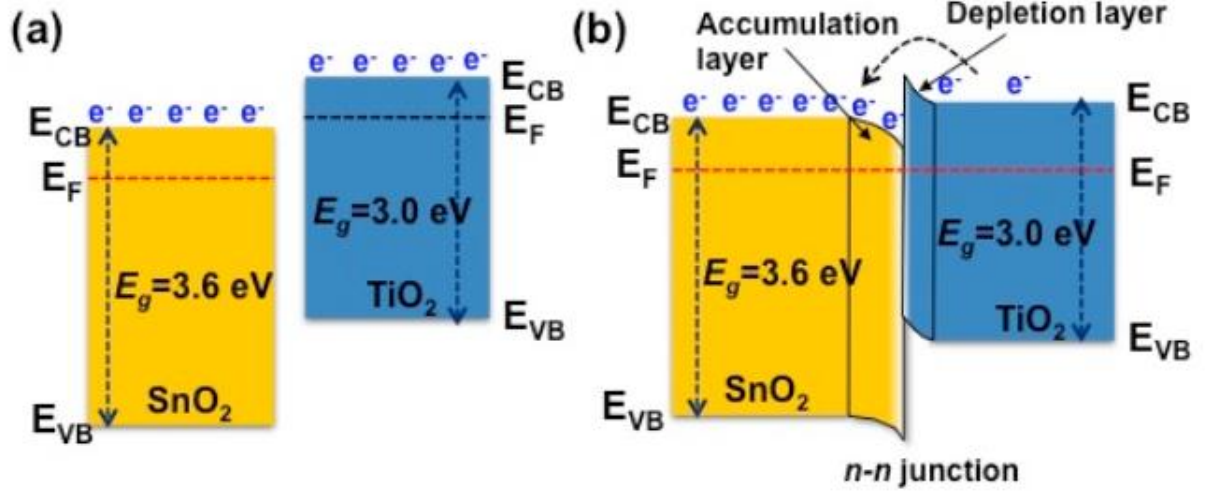


Figure 2.1: Energy-band diagram for the TiO<sub>2</sub>-SnO<sub>2</sub> composite system. (Thangadurai and Mulmi, 2011)

Higher rate of electron transfer increases the conductivity of sensing material and enhances the sensor output (Vaezi et al., 2012). The transport of electron from TiO<sub>2</sub> to SnO<sub>2</sub> promotes oxygen pre adsorption at the surface of SnO<sub>2</sub> grains which is highly desirable, as SnO<sub>2</sub> grains are assumed to be more suitable for oxygen adsorption. The efficiency of the O<sup>-</sup> adsorption process and the number of adsorption sites is greatly increased with adequate concentration of electrons (Lyson-Sypien et al., 2017). An n-type semiconductor, being discussed in our study, SnO<sub>2</sub>/TiO<sub>2</sub> sensing material possesses majority charge carriers of electrons, whereby when reacts with reducing gases, experiences increment in conductivity and vice versa for oxidizing gas (Fine, 2010). However, the study also points out the importance in determining the appropriate TiO<sub>2</sub> wt% doping required to reduce cross-sensitivity towards without compromising band gap energy (Reduction of band gap by 0.45 eV when Ti-content is increased by 5.5%) since TiO<sub>2</sub> has lower conductivity and sensitivity towards most analytes (Tricoli et al.,

2009), thus the author reckon the need of synthesizing a desired ratio of composite Semiconductor Metal Oxide (SMO) sensor for environmental applications.

### 2.3 Effect of TiO<sub>2</sub> wt% doping on SnO<sub>2</sub> on ethanol vapor concentration

Although SnO<sub>2</sub> based active materials possess high sensitivity towards volatile organic compound (VOC), in our case, ethanol, however, SnO<sub>2</sub> gives out poor sensor response in low gas concentration. This is supported by study done by (Zeng et al., 2010), whereby pure SnO<sub>2</sub> sensor response is almost halved compared with TiO<sub>2</sub> doped SnO<sub>2</sub> sensors when tested with ethanol at 633K. This is because at a low concentration of gas, lower coverage of gas molecules are covered on a fixed surface area and hence lower surface reaction occurs. An increase in gas concentration would eventually increase the surface reaction due to a larger surface coverage. Nevertheless, approaches of doping metal oxides and noble metals has proven to be futile as these sensors could actually able to give out better sensor output in gas concentration as low as 50ppm and improved sensor output in higher concentration. A research paper done by (Kanan et al., 2009) has proven that the doping of La<sub>2</sub>O<sub>3</sub> to SnO<sub>2</sub> using a 0.5 M La (NO<sub>3</sub>)<sub>3</sub> aqueous solution showed an increase in response to acetone (~3.6 times) and ethanol (~5.5 times). Besides, the doping of a similar n-type ZnO<sub>2</sub> to SnO<sub>2</sub> done by (Tharsika et al., 2014) proves that SnO<sub>2</sub>-core/ZnO-shell hierarchical nanostructures has higher sensitivity to ethanol than just SnO<sub>2</sub> nanowires in every tested concentration of ethanol from 20 to 400ppm.

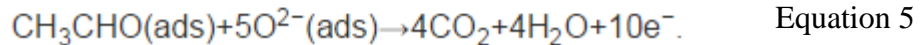
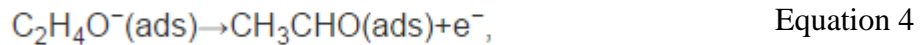
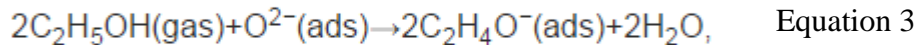
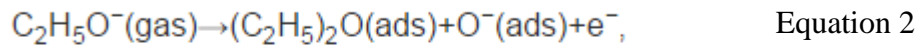
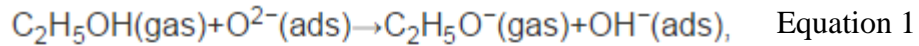
The doping of metal oxides or noble metal on SnO<sub>2</sub> produces smaller grain size with larger surface area that provides higher surface activity for adsorption of oxygen

and its reaction with test gas. Higher rate of O<sub>2</sub> adsorption the sensor surface creates a larger difference in the electrical conductivity of the sensor and enhances sensor response (Chikhale et al., 2014). A study done by (Chikhale et al., 2014) on pure SnO<sub>2</sub> and various doped Fe on SnO<sub>2</sub> of 2% and 4 mol% respectively shows, that 2 mol% Fe doped SnO<sub>2</sub> shows highest sensor response towards ethanol at 300°C. In the exact study, the average crystalline structure of pure SnO<sub>2</sub>, 2 mol% Fe-doped SnO<sub>2</sub> and 4 mol% Fe-doped SnO<sub>2</sub> are 17, 10 and 8 nm. Although has lowest crystalline structure, Higher Fe-sites concentration on the surface of 4 mol% Fe-doped SnO<sub>2</sub> has covered SnO<sub>2</sub> base material that is responsible for effective adsorption–desorption processes of gases and hence decreases the sensor response Thus, the need to find ideal TiO<sub>2</sub> wt% doping is necessary for the optimization of sensor response.

A study done by Zeng et al., 2010, shows that the grain size of TiO<sub>2</sub> doped SnO<sub>2</sub> reduces from 20 to 10 nm when the TiO<sub>2</sub> doping concentration increases from 0.1 to 0.8. The diffusion of TiO<sub>2</sub> into grain boundaries of the polycrystalline SnO<sub>2</sub> prohibits the growth of the grains. The restrained growth of the grains allows maximization of O<sub>2</sub> adsorption on surface due to higher specific surface area. The TiO<sub>2</sub>-doped polycrystalline SnO<sub>2</sub> sensors exhibits higher *S*/*ss* (Sensitivity per specific surface area) compared to pure SnO<sub>2</sub>, indicating that small amounts of Ti dispersion on grain boundaries, directly or indirectly affects the density of centers active for the gas adsorption, increase the surface energy and the effectiveness of these centers by the surface amorphization.

The ideal TiO<sub>2</sub> doping into SnO<sub>2</sub> can be best explained through band theory, whereby the pre-adsorbed oxygen could give rise to a depletion layer near to the surface

of *n*-type semiconducting oxides, which forms a band bending around surface. This band bending tends to enlarge the energy barrier and the resistance of composite. Electron transfer from TiO<sub>2</sub> to SnO<sub>2</sub> occurs due to higher conduction band (CB) minimum and valence band (VB) of TiO<sub>2</sub> than SnO<sub>2</sub>. The hetero-junctions may be formed at grain boundaries and maintain till the electron affinity of adsorbed oxygen reaches the same level as that of TiO<sub>2</sub>-SnO<sub>2</sub> due to high work function by SnO<sub>2</sub> and strong electron affinity by TiO<sub>2</sub>. Oxygen adsorption occurs rapidly on the surface. The strong electron negativity of the adsorbed oxygen traps the conduction band (CB) electrons and reduces electric conductivity through the oxide. When a reductive gas, in our case, ethanol, reacts with the surface, chemical reactions that would occur between ethanol molecule and the pre-adsorbed oxygen are shown below (Zeng et al., 2010):



#### 2.4 Effect of TiO<sub>2</sub> wt% doping on pure SnO<sub>2</sub> on different humidity of ethanol vapor

Tin oxide's strong cross-sensitivity to humidity restricts its ability in detection of ethanol vapor in high humidity. Due to strong cross-sensitivity to humidity, the rate of adsorption of hydroxyl group on the thick film is higher thus prohibiting electron transfer to sensing layers. The sensitivity of metal oxide sensors gradually decreases as the following occurs (Yin et al., 2010):

1. The reaction between the surface oxygen and the water molecules decreases baseline resistance of the gas sensor that results in a decrease of the sensitivity.
2. Lesser oxygen species chemisorbed on the SnO<sub>2</sub> surface due to the reduction in the surface area that is responsible for the sensor response as the adsorption of water molecules builds up.
3. Water molecules prohibit the adsorption of target gas. The superficial transfer of the target gas on the SnO<sub>2</sub> surface becomes harder, thus the sensitivity decreases and the response and recovery times increase.

The doping of metal oxide that has lower cross sensitivity than SnO<sub>2</sub> enhances crystal defects and minimizes the adsorption of hydroxyl group on the surface of thick film (Tricoli et al., 2009). The author opt to use the doping of Titanium Dioxide, TiO<sub>2</sub> since Ti has minimum cross-sensitivity towards humidity and widely used as humidity sensors that are used in for removing systems on the rear windows ,and white wood coating (Afuyoni et al., 2011). A study done by (Tricoli et al., 2009) on pure SnO<sub>2</sub> and TiO<sub>2</sub>-doped SnO<sub>2</sub> with different Ti- content (%) found that cross sensitivity to humidity increases by 18% in Ti-content (4.6%) compared to increase by 74% in pure SnO<sub>2</sub> when the relative humidity of ethanol vapor is increased from 0% to 60%. However, the drawback in the study is the increase of cross-sensitivity when Ti-content increases for all the relative humidity parameters tested that contradicts the knowledge related to the research.

## 2.5 Effect of TiO<sub>2</sub> wt% doping on pure SnO<sub>2</sub> on operating temperature of ethanol vapor.

Another important parameter that is investigated in this study is the effect of TiO<sub>2</sub> doping (on SnO<sub>2</sub>) on the operating/working temperature of the ethanol vapor. Amidst, its high sensitivity towards most of the analytes, SnO<sub>2</sub> based sensors are restricted to only lower working temperature due to its thermal degeneration nature that occurs above 400°C thus dampening the sensing performance. TiO<sub>2</sub> doping on SnO<sub>2</sub> is recommended because TiO<sub>2</sub> is stable at higher temperature. According to study done by (Vaezi et al., 2012), TiO<sub>2</sub> doping on SnO<sub>2</sub> is able to work in higher temperature, because more heat energy is required for electrons from TiO<sub>2</sub> to transfer to SnO<sub>2</sub>, that increases the conductivity of sensing material, due to TiO<sub>2</sub> high stability in high temperature. However, the result obtained in the study contradicts to the statement above, whereby Ti-doped SnO<sub>2</sub> thick film (Ti:Sn weight ratio of 1:1 and 1:2) sensitivity reduces beyond 250°C while, pure SnO<sub>2</sub> exhibits increasing sensitivity beyond 250°C when tested with 1000 ppm of ethanol, indicating that further investigation is needed. In contrast to the study, another research paper (Wang et al., 2015) has shown higher sensitivity in TiO<sub>2</sub> doped SnO<sub>2</sub> than both pure TiO<sub>2</sub> and SnO<sub>2</sub> up to 350°C when tested with 500 ppm acetone gas. The increment of working temperature of SnO<sub>2</sub> through foreign metal oxide doping is further supported by study done by (Bagal et al., 2012) on pure SnO<sub>2</sub> and various wt% Palladium (Pd) doped SnO<sub>2</sub>, whereby, the highest Pd wt% of 3 shows higher sensitivity, while pure SnO<sub>2</sub> shows lowest sensitivity in all tested temperatures, when tested with 500 ppm Liquefied Petroleum Gas (LPG). Another research paper done by Chikhale et al., 2014 that studies on pure SnO<sub>2</sub> and various mol% Iron (Fe) doped SnO<sub>2</sub>, shows doping of foreign metal oxide increases sensitivity in higher



temperature compared to pure SnO<sub>2</sub>. However, the author opt to find the optimum wt% TiO<sub>2</sub>-content required for highest sensitivity because the study (Chikhale et al., 2014) indicates that highest foreign metal oxide doping in SnO<sub>2</sub> (in this case, mol% Fe) does not assure highest sensitivity as working temperature increases, as 2 mol% doped Fe shows higher increase in sensitivity than 4 mol% Fe when tested with 2000ppm ethanol.

## 2.6 Screen-printing method

The author opt to use thick film technology using screen printing method, whereby calcinated powders (active material) are mixed with organic binder and solvent with the ratio of 40:5:55 (active material: organic binder: solvent) to form paste to be printed on aluminate substrate for gas sensing measurement. Screen-printing working principle is by forcing an ink/paste through a porous layer or mesh that ideally forms the required layer on the substrate. The ink essentially holds the material to be deposited, dispersed in a viscous vehicle/organic binder and is printed on of the substrate. Once the ink is has been deposited, the print can be heated to remove the vehicle, leaving a solid material on the target area of printing. Figure below shows the general form of commercial metal oxide semiconductor gas sensors.

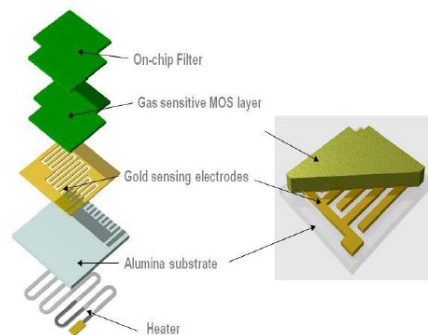


Figure 2.2: Physical form of screen-printed SMO gas sensors (Fine, 2010).

Below are the advantages of screen printing approach (Moina, 2005):

1. The particle size can be varied by altering preparative conditions
2. Different blends of metal clusters can be formulated, opening up the possibility of fine-tuning the sensitivity of the sensors towards different gases.
3. The uncertainties concerning the chemical nature, particle size and localization of the catalyst in the fabricated sensor are considerably diminished.

Other advantages include manufacture of multiple layers on one or both side of substrate, low cost, high sensitivity, high mechanical and chemical stability (Ehsani et al., 2016).

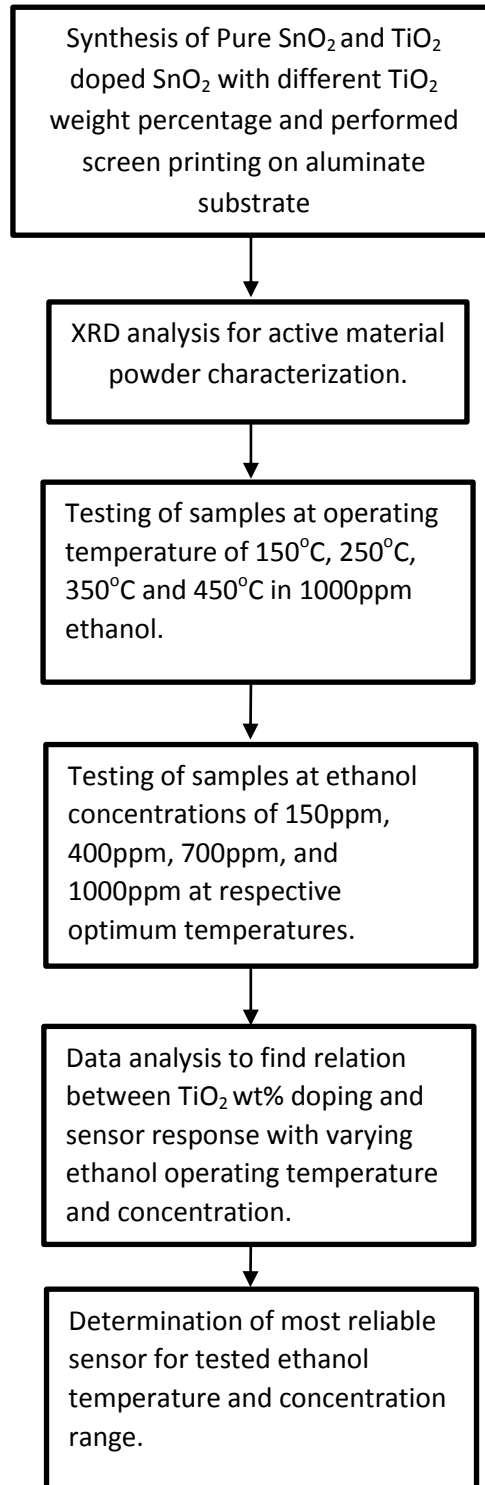
## 2.7 Sol-gel and co-precipitation method

Pure SnO<sub>2</sub> is prepared using stannic chloride, SnCl<sub>4</sub>.5H<sub>2</sub>O as tin precursor via co-precipitation method because it improves the surface area of active material, simple and inexpensive (Bagal et al., 2012). Sol-gel method approach is used in preparing TiO<sub>2</sub> doped SnO<sub>2</sub> active material powder due to its simplicity, lower cost per area coating, minimum process hazards and eliminates the necessity of a costly vacuum system (Bhasha et al., 2015).

## CHAPTER THREE

### MATERIALS AND METHOD

#### 3.1 Introduction



### 3.2 Materials

Table below shows the materials used in the experiment.

Table 3.1: Specification of material used.

Material	Specification	Manufacturer / Source
Titania nanoparticles	98% purity	BDH Laboratory Supplies
Ammonia solution, NH <sub>4</sub> OH	25 wt% solution	Merck KGaA
Ethanol absolute	99.98% v/v	HmbG Chemicals
Stannic chloride, SnCl <sub>4</sub> .5H <sub>2</sub> O	98+%, extra pure	AEROS Organics
Hydroxypropyl cellulose (organic binder)	20 mesh particle size (99% through)	ALDRICH Chemistry
Deionized water		Environmental Laboratory, School of Chemical Engineering.

### 3.3 Active material synthesis.

#### 3.3.1 Preparation of TiO<sub>2</sub> doped SnO<sub>2</sub> powder.

The approach used is sol-gel method and adopted from (Vaezi et al., 2012). Since the effect of various weight percentages TiO<sub>2</sub> doping on pure SnO<sub>2</sub> were examined, different amount of TiO<sub>2</sub> precursor is added and explained in the table below. The amount of

SnO<sub>2</sub> precursor is maintained in all TiO<sub>2</sub> doped SnO<sub>2</sub> sample proportion, which is 0.878 g.

Table 3.2: Different TiO<sub>2</sub> wt% doping on SnO<sub>2</sub> powder synthesized

TiO <sub>2</sub> wt%	Symbol denotation	Titania particles (g)	Stannic chloride, SnCl <sub>4</sub> .5H <sub>2</sub> O (g)
20	S2	0.219	0.878
40	S3	0.585	0.878
60	S4	1.317	0.878

Mass of titania powder according to samples are dissolved in 40mL of deionized water. Then, SnCl<sub>4</sub>.5H<sub>2</sub>O diluted with 25 ml de-ionized water, is poured into the solution. 15 mL of NH<sub>4</sub>OH solution is added gradually using a burette, forming white slurry. After stirring for 24 h, the resulting product is filtered and dried at 60°C. Since neither centrifugation nor filtration method can successfully separate Ti-doped SnO<sub>2</sub> powder from the white slurry solution. Thus, the white slurry is dried at 100°C overnight to evaporate the remaining water molecules, leaving only the powder sediment in the beaker. The obtained powder then calcined to 500°C in 1 hour.

### 3.3.2 Preparation of pure SnO<sub>2</sub> powder.

The approach is adopted from (Bagal et al., 2012), whereby, 0.025M of SnCl<sub>4</sub>.5H<sub>2</sub>O is prepared by dissolving 0.878g in 100 mL of deionized water. The solution is continuously stirred in medium RPM with gradual addition of NH<sub>4</sub>OH until the pH of solution reaches 8. A white chalky solution will be formed. The solution is then filtered to obtain SnO<sub>2</sub> gel and is washed for three times using 25mL of ethanol

each. The washed gel is then dried overnight in the temperature of 60°C and further calcined at 600°C for 2 hours. The complication faced in these steps is the conventional filtration method using filter paper and conical flask takes a very long time to filter SnO<sub>2</sub> gel, thus, in order to save time, vacuum filtration method is adopted.

#### 3.4 Preparation of pure SnO<sub>2</sub> and Ti doped SnO<sub>2</sub> thick film ethanol gas sensor.

The thick film of calcinated powder is fabricated through screen printing method as performed by (Masayoshi Nitta et al., 1979). The calcinated powder is mixed with organic binder with the ratio of 40:5:55 (active material powder: organic binder: ethylene glycol) totaling up to 10g of paste to be screen printed by 5 layers on 10mm by 10mm aluminate substrate with a mesh screen. Each layer is dried for 10 minutes before another layer is printed and after 5<sup>th</sup> layer, the substrate is dried in 60°C for 3 hours. The prepared thick films are calcined at 400°C for 1 hour for the removal of organic binder.

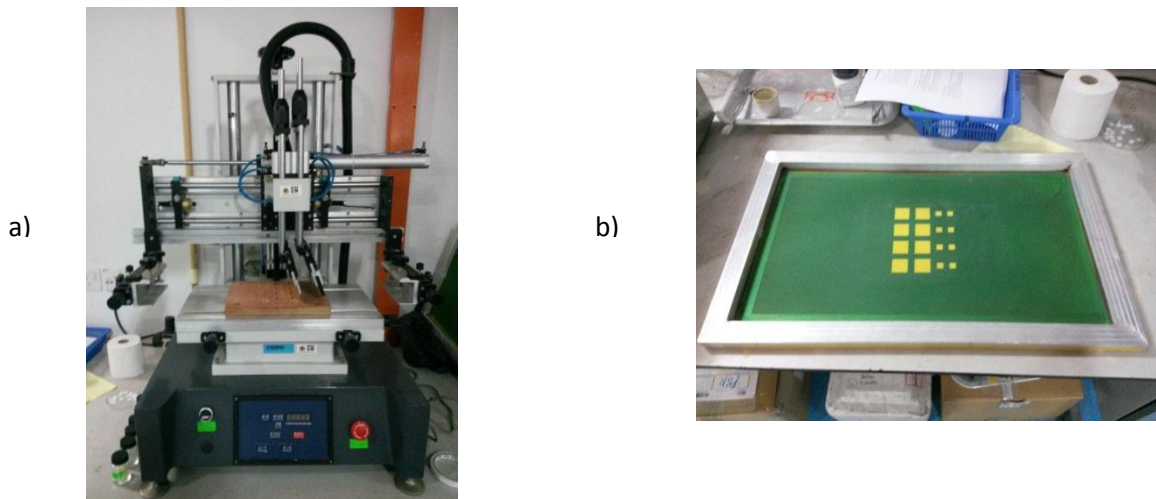


Figure 3.1: (a) Semi-auto screen printing machine. (b) Mesh screen

### 3.5 Experimental design

Two parameters that involved are operating temperature of ethanol vapour and concentration of ethanol vapour. The effect of TiO<sub>2</sub> weight % doping of 20 %, 40% and 60% on pure SnO<sub>2</sub> on these two parameters are studied. The optimisation of ethanol operating temperature is performed by running four different sensors with different TiO<sub>2</sub> wt% doping and pure SnO<sub>2</sub> on 1000ppm of pure ethanol. The testing of sensors with different ethanol concentration is performed on respective optimum temperatures obtained. Each run for both optimization of temperature and concentration is done for 1200s and 800s. Thus, a minimum of two cycles are obtained for the determination of sensor sensitivity.

### 3.6 Equipment and instrumentation

#### 3.6.1 Sensor characterization

##### 3.6.1(a) X-ray Diffraction (XRD)

The X-ray diffraction (XRD) pattern of the samples was done on Siemens 2000X system in School of Minerals and Material Resources. The system uses Cu-K $\alpha$  radiation in range of 1-5 $^{\circ}$  with a step size of 0.01 $^{\circ}$  at 2-theta values between 20 $^{\circ}$ C and 80 $^{\circ}$ C. The XRD patterns of pure SnO<sub>2</sub> and various wt % of TiO<sub>2</sub> doping on pure SnO<sub>2</sub> are shown in chapter 4. XRD is performed to determine the phases of chemical compound present in the surface of substrate and crystalline size of active material.

### 3.6.2 Sensor Measurement Unit

A gas sensing experimental rig is set up as shown in the schematic diagram in Figure 3.1. The equipment used includes purified air and ethanol vapor storage tanks, control valves, mixer, gas chamber, heater, thermocouple, electrometer and temperature controller. In the gas chamber, the sensor is connected to an electrometer by a pair of clips. The heater is allowed to heat up to 150 °C and the temperature is measured by a thermocouple. The purified air inlet valve is opened and its flow rate is set to 300 ml/min while the ethanol vapor inlet valve is opened with its concentration being set to the desired concentration using mass valve controller. A computer which is equipped with the software Xlogger is connected to the electrometer and is used for data acquisition, storage and plotting in real time for the analysis of sensitivity of gas sensor. After the operating temperature reaches steady state, a constant voltage of 5 V is supplied. The DC resistance of the gas sensor is measured for every second by the electrometer. The data collected is transferred into the computer and saved. The sensitivity analysis is calculated automatically by the software. The sensor performance testing is repeated at operating temperature of 150°C, 250°C, 350°C and 450°C. Then the testing is carried out for different ethanol concentration from 150 to 1000ppm at the optimum temperature.



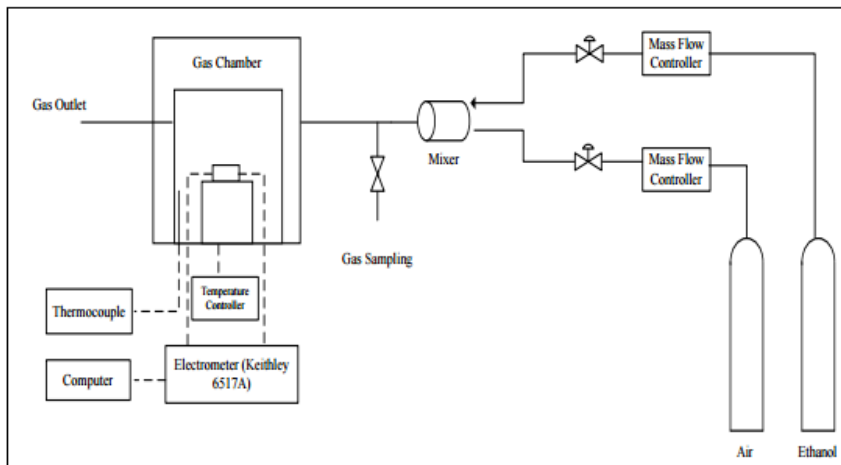


Figure 3.2: Schematic diagram of the gas sensor rig.



Figure 3.3: Actual set-up of sensor measurement rig

## CHAPTER FOUR

### RESULTS AND DISCUSSION

#### 4.1 Introduction

This chapter presents the experimental results and discussion and consist of three main sections. The first section illustrates the experimental design that covers the preparation of different sensors for experimental purpose as well as the parameters involved. The second and third section respectively discusses the characterization of the sensors and study on optimisation of parameters involved.

#### 4.2 Sensor characterization

##### 4.2.1 XRD Analysis

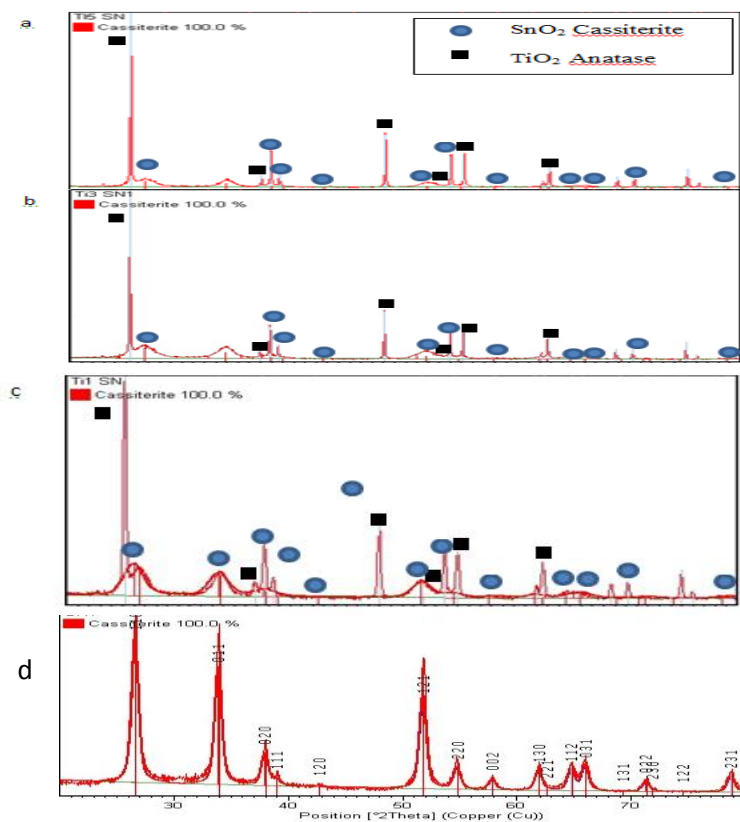


Figure 4.1: XRD patterns of the samples: (a) 60 wt%  $\text{TiO}_2$ -40 wt%  $\text{SnO}_2$ , (b) 40 wt%  $\text{TiO}_2$ -60 wt%  $\text{SnO}_2$ , (c) 20 wt%  $\text{TiO}_2$ -80 wt%  $\text{SnO}_2$ , (d) Pure  $\text{SnO}_2$ .

The X-ray diffraction (XRD) pattern of the samples was obtained on Siemens 2000X system using Cu-K $\alpha$  radiation in range of 1-5 $^{\circ}$  with a step size of 0.01 $^{\circ}$  at 2-theta values between 20 $^{\circ}$ C and 80 $^{\circ}$ C. The XRD patterns of pure SnO $_2$  and various wt % of TiO $_2$  doping on pure SnO $_2$  are shown in Fig 4.1. All the diffraction patterns show characteristic SnO $_2$  peaks obeying cassiterate structure as accordance to JCPDS file No. 41-1445 (Wang et al., 2015). For TiO $_2$  doped SnO $_2$  sensors the spectrum of x-ray diffraction indicates the presence of TiO $_2$  in anatase form with diffraction angles {25.2 – 37.9 – 47.8 – 53.8 – 55 – 63} degree meeting the indexes of the following levels : (101 – 004 – 200 – 105 – 211 – 204 ) respectively as accordance to (JCPDS file No. 21-1272) (Afuyoni et al., 2011; Wang et al., 2015). It is observed that with increasing TiO $_2$  wt% doping, the SnO $_2$  peaks broaden and experiences lower relative intensity, indicating reduction in the crystallite size due to incorporation of TiO $_2$  into SnO $_2$  lattice structure (Kusior et al., 2013). A smaller crystallite size provides a larger surface area for exposure to the test gas, thus enhancing sensor surface reaction with target gas, thereby increasing the response (Bagal et al., 2012). Extra peak corresponding to TiO $_2$  in the XRD pattern was obtained which may due to higher concentration of TiO $_2$  or unsuccessful substitution of TiO $_2$  at Sn site.

Table 4.1: Crystallite size of samples using Rietveld refinement

Samples	Crystallite Size (nm)
Pure SnO $_2$	11.97
20 wt% TiO $_2$ -80 wt% SnO $_2$	4.04
40 wt% TiO $_2$ -60 w% SnO $_2$	3.94
60 wt% TiO $_2$ -40 wt% SnO $_2$	3.69